Technische Universität Braunschweig

Institute of Operating Systems and Computer Networks

No-Cost Distance Estimation Using Standard WSN Radios

Georg von Zengen and Yannic Schröder and Stephan Rottmann and Felix Büsching and Lars C Wolf

Authors post-print published on 2020-07-22
Originally published in *The 35th Annual IEEE International Conference on Computer Communications (INFOCOM 2016)*
Publisher version available at http://ieeexplore.ieee.org/document/7524540/?arnumber=7524539
DOI: 10.1109/INFOCOM.2016.7524540

Abstract:

Being able to determine the location of a node is of great advantage in many IoT and WSN applications. For example in health care scenarios or for autonomous configuration of IoT setups this information can be useful. One of the key challenges in localization is to estimate the distance between nodes. Most present indoor localization systems require additional hardware to perform this estimation, that is costly in terms of money and energy consumption. To overcome this disadvantage, we developed a system which is able to perform distance measurements without adding any extra hardware and costs. It is based on phase measurements performed by the IEEE 802.15.4 transceiver chip that is normally solely used to realize communication. In the evaluation we investigate the performance of our system in different real world environments that are typical for IoT and WSN setups.

No-Cost Distance Estimation Using Standard WSN Radios

Georg von Zengen, Yannic Schröder, Stephan Rottmann, Felix Büsching and Lars C. Wolf
Institute of Operating Systems and Computer Networks
Technische Universität Braunschweig
Email: [vonzengen|schroeder|rottmann|buesching|wolf]@ibr.cs.tu-bs.de

***Abstract*—Being able to determine the location of a node is of great advantage in many IoT and WSN applications. For example, in health care scenarios or for autonomous configuration of IoT setups this information can be useful. One of the key challenges in localization is to estimate the distance between nodes. Most present indoor localization systems require additional hardware for this estimation which is costly in terms of money and energy consumption. To overcome this disadvantage, we developed a system which is able to perform distance measurements without adding any extra hardware and costs. It is based on phase measurements performed by the IEEE 802.15.4 transceiver chip that is normally solely used to realize communication. In the evaluation we investigate the performance of our system in different real world environments that are typical for IoT and WSN setups.**

I. Introduction

In many Internet of Things (IoT) and Wireless Sensor Network (WSN) applications knowing the distance between nodes brings great benefits. The use cases of this knowledge range from packet routing to location tracking for patients in health care facilities like retirement homes. Especially for the localization use cases most of the existing approaches use specialized hardware to perform the distance measurement. We propose InPhase, a system that is able to determine the distance without adding any extra hardware to an existing WSN. To achieve this we utilize Commercial Off-The-Shelf (COTS) radio chips that are able to perform phase measurements on their communication signals. Hence, our system is much more cost efficient which makes it also very attractive for large IoT setups. Nonetheless, InPhase does not lack measurement accuracy. The median error over all tested scenarios is 30 cm for our system. We outperform the competing Ranging Toolbox (RTB) by 33 %.

As stated by Boukerche et al. [2] localization is a combination of three separate tasks: distance estimation, position computation, and the localization algorithm. In this paper we focus on the distance estimation. Therefore, we present related work focused on this task in Section II. In Section III challenges we work on and the theoretical background of phase measurements are explained in detail. The description of our system is given in Section IV. Afterwards we present our evaluation and the results in Section V. In Section VI we conclude the paper.

II. Related Work

In this section, we focus on distance estimation since it is the most difficult task in localization. Well-known methods for distance estimation can be divided into four groups: Received Signal Strength Indicator (RSSI)-based, time-based, angle-based, and phase-based measurements. Different requirements in hardware result in different additional costs.

A. RSSI-based measurements

In an ideal free space scenario, the RSSI value would decrease with increasing distance and could be used to calculate the distance between nodes. Even in outdoor scenarios where a direct line of sight (LOS) is available, multipath propagation exists due to reflections which makes the RSSI value unusable as a direct indicator for the distance. Other problems arise from environmental influences that cannot be controlled in most cases, such as humidity [7]. Interpreting low RSSI values originating from these effects as long distances may result in huge measurement errors.

Many RSSI-based systems rely on so-called fingerprinting [5]. For example, RSSI values of Wireless Local Area Network (WLAN) stations in range can be recorded and stored in a database that can be used later to estimate the position of a node. When the RSSI values diverge from the database, this method may generate incorrect positions. Changes of the RSSI value can originate from reflections on moving objects or simply new or deactivated stations.

B. Time-based measurements

Two different methods need to be distinguished when utilizing the transit time of radio signals to estimate the distance between nodes: Time of Arrival (ToA) and Time Difference of Arrival (TDoA) [2]. When using ToA, the transit time of the signal is measured directly. This requires highly synchronized clocks to calculate the time between departure and arrival. TDoA measures the difference in arrival times between two receiving nodes or multiple signals with different propagation speeds at a single node. When measuring the TDoA between two nodes, synchronized clocks are required like for ToA. The latter variant is used by the sensor node “Medusa” [11]. The authors use the difference in propagation time between radio waves and ultrasound (US). Due to the low range of US, the system is only able to handle distances up to three meters.

Larger distances can be obtained using other US transceivers, that have a higher demand of energy.

C. Angle-based measurements

Positioning systems based on angle measurements either compare the RSSI of multiple receivers with different predominant directions of antennas or rely on propagation delays at several points in a receiver array. The "Cricket Compass" [10] utilizes the angle to a sender. Differences in reception times of an US pulse at multiple receivers in a plane are recorded and calculated into the angle between the plane and the transmitter. Having multiple angles, it is possible to calculate the position in space. Due to the utilization of US, this system suffers from the same restrictions as "Medusa".

D. Phase-based measurements

Electromagnetic near field measurements [12] are based on the fact that magnetic and electrical field components of electromagnetic transmitters are not in phase in their near field. If a receiver measures both components individually, the known wavelength of the signals allows the calculation of the distance to the transmitter. The size of the near field depends on the wavelength of the signal. A low frequency and thus a large wavelength is required for precise measurement. The long antennas needed for such wavelengths are a great drawback for tiny sensor nodes. Additionally, special receiver hardware is required for this method.

Another option to utilize phase based measurements for distance estimation is to compare the phasing of signals with different frequencies at the receiver. A solution with transceivers able to send and receive at two frequencies simultaneously has been proposed [8]. The phasing of the signals transmitted is known to the receiver, additional synchronization of clocks is not required. The maximum range that can be measured using this method only depends on the two frequencies chosen. For example, if a frequency offset of 2 MHz has been chosen, distances up to 150 m can be measured. Greater distances can not be identified unambiguously.

The basic method for distance estimations based on phase measurements has been proposed by Kluge et al. [6] and is called Active Reflector (AR). By performing bidirectional phase measurements at different frequencies the disturbing influence of not synchronized clocks is eliminated. Afterwards, Pelka et al. [9] investigated the theory behind the AR in detail. However, the approach presented by them suffers from the trade-off between accuracy and maximum measurement range.

In this paper we present a novel approach based on the idea of the AR method. Compared to the works of Kluge and Pelka, our approach overcomes the trade-off and is able to achieve a better accuracy. We provide new contributions to the way AR measurements are performed and how the results of these measurements are processed to determine the distance. We apply calculations on the data to determine the Power Spectral Density (PSD) of sampled data. This allows us to get a qualification of the measurement's accuracy in addition to more accurate distances.

III. Phase Measurement Basics

In this section we give a short overview over the challenges of distance estimation using phase measurements, the AR method and our novel approach to determine the distance based on the PSD of the sampled data.

A. Challenges

A distance estimation based on phase measurements is theoretically possible as Equation 1 by Kluge et al. [6] states. By measuring two phases (φ_1 and φ_2) of a signal at two different known frequencies a distance can be calculated.

$$d = \frac{(\varphi_2 - \varphi_1) \cdot c}{2\pi \cdot \Delta f} \tag{1}$$

Δf represents the difference between the two frequencies, while c is the propagation speed, hence the speed of light.

Modern IEEE 802.15.4 transceiver chips as the *AT86RF233* by *Atmel* feature a Phase Measurement Unit (PMU) to measure the received signal's phase. However, the phase must always be measured to a reference signal. If sender and receiver do not use the same reference signal the outcome of a measurement is meaningless. Maintaining the needed synchronization is nearly impossible in wireless networks. The AR method [6] relaxes the requirement for the synchronization.

The transceiver chip's PMU has a finite angular resolution. When measuring only two phases as in [9] a trade-off between good resolution in the resulting distance estimation and the maximum measurable distance needs to be employed.

We propose a system which overcomes these disadvantages by using more than just two frequencies from the Industrial Scientific Medical (ISM) band. Our system uses the whole available ISM band and conducts as many measurements as possible by using the smallest frequency difference available. With this approach we impose no trade-off between large distances and accuracy as we no longer rely on only one phase difference between two frequencies but can estimate the slope over a multitude of phase differences. This also compensates for disturbed measurements arising from occupied frequencies.

B. Theoretical Background

A Phase Measurement Unit (PMU) measures the phase angle φ between an internal reference frequency and the received base band signal. Therefore, the time Δt between the rising edge of both signals is measured. If the period T is known, the phase angle φ can be calculated as follows:

$$\varphi = 2\pi \cdot \frac{\Delta t}{T} \tag{2}$$

For the *AT86RF233* the measured value is the term $\frac{\Delta t}{T}$, that is represented in an 8 bit wide integer. Due to Offset Quadrature Phase-Shift Keying (O-QPSK) that is used for regular IEEE 802.15.4 operations the measurement cannot be performed during normal data transfer. Therefore, the transmitting *AT86RF233* needs to be set into a mode where it transmits an unmodulated sine signal.

To measure the distance between the transmitter and the receiver using the phase angle between the receiver's reference

clock and the received signal, both reference clocks have to be exactly synchronous. Exact synchronization in WSNs is a nearly impossible task. The AR method [6] is able to measure the phase angle without synchronized reference clocks. The two involved nodes are called initiator and reflector. The initiator is the node that needs to know its distance to the reflector. In the first step both nodes set their Phase Locked Loop (PLL) to f_1 which was negotiated between both nodes before. While the initiator transmits an unmodulated signal, the reflector measures the phase angle φ_{R_1}. Then, the nodes change their roles and the reflector transmits the unmodulated signal while the the initiator measures the phase angle φ_{I_1}. The same mechanism is repeated on frequency f_2 and φ_{R_2} and φ_{I_2} are measured. Now the measurements from the reflector are transmitted to the initiator. By subtracting φ_{R_2} from φ_{I_2} and φ_{R_1} from φ_{I_1}, the effect of non-synchronous reference clocks is eliminated.

$$\Delta\varphi = (\varphi_{I_2} - \varphi_{R_2}) - (\varphi_{I_1} - \varphi_{R_1}) \tag{3}$$

The distance between both nodes can be calculated using Equation 4.

$$d = \frac{\Delta\varphi}{\Delta f} \cdot \frac{c}{\pi} \tag{4}$$

According to Kluge et al. [6] it is important that the time between the measurement of φ_{R_1} and φ_{I_1} is constant, the same applies for φ_{R_2} and φ_{I_2}. Thus, it is necessary that an implementation of the AR method ensures a constant time between these measurements.

IV. System Design

The proposed system is integrated into the Contiki operating system [4]. From the user perspective the distance measurement can be used like all other sensors in Contiki using the sensor interface. Therefore, it can easily be used in all layers of the operating system, from user applications to networking protocols.

We implemented the AR method [6] as described in Section IV-A. The implementation uses a multitude of frequencies in contrast to only two frequencies used by Pelka et al. [9] to mitigate harmful effects of other radio signals. Our novel approach to calculate the distance based on such measurement is described in Section IV-B.

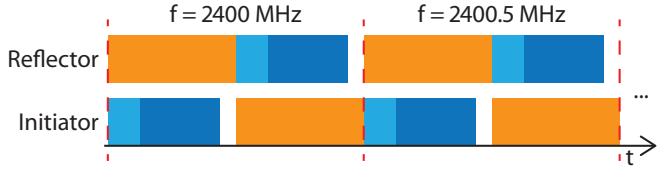

Fig. 1. Sequence of an Active-Reflector-Measurement

A. Phase Difference Measurement

Figure 1 gives an overview of the procedure of a measurement. After both nodes have agreed to perform a measurement, the reflector starts to transmit an unmodulated signal for a certain time (orange boxes). Meanwhile the initiator waits for a guarding time (light blue boxes) and starts sampling phase measurements afterwards (dark blue boxes). This guard time is needed to ensure the reflector has started to transmit the unmodulated signal. Once the initiator has finished its measurement, both nodes switch roles. Here the loose synchronization is needed since the PLLs of the node must not be recalibrated between the measurements of the initiator and the reflector. Therefore, no packet can be transferred to indicate the role switch. After both nodes have switched roles a new measurement is performed. Now the initiator knows the phase angle φ_{I_1} and the reflector φ_{R_1}; the values are stored locally.

At least two measurements on different frequencies are needed for the distance estimation, so both nodes switch to a different frequency. On this frequency both nodes measure the phase angles as described above, so φ_{R_2} and φ_{I_2} are known. Theoretically these two measurements would be sufficient to calculate the distance (see Equations 3 and 4). However, InPhase measures phase angles over all frequencies in the ISM band to mitigate erroneous measurements. This sequence of measurements and frequency switches is performed in steps of $500\,kHz$. We chose $500\,kHz$ because it is the smallest step configurable for the used transceiver chip. It would be desirable to choose even smaller steps as this would allow to measure larger distances [9].

Subsequently the reflector transmits all stored values of φ_R to the initiator. According to Equation 3 the initiator performs Equation 5 for all stored values, where N is the number of stored values.

$$\varphi_x = \varphi_{I_x} - \varphi_{R_x} \forall x \in \{1, \ldots, N\} \tag{5}$$

φ_x is now the doubled phase angle, but free from errors caused by the asynchronicity of the PLLs. It is doubled since the signal travelled twice the actual distance due to the AR method.

B. Distance Estimation

According to Equations 3 and 4, the distance can be estimated from the slope of φ_x over the different frequencies. Figure 2 shows a phase response Φ measured by our system.

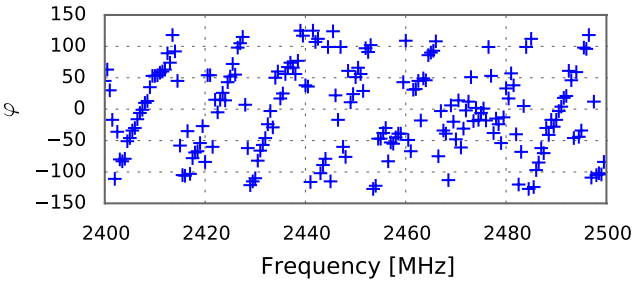

Fig. 2. Raw phase response measurement Φ

The phase response Φ resembles a saw tooth signal. The signal is plotted over the measured frequencies and shows phase angles that wrap around every 360°. Its slope is proportional to the distance between initiator and reflector.

Not all measurements fit the saw tooth well. This is caused by interference with other radio signals on the respective frequencies. The PMU is unable to distinguish the measurement signal from any other radio wave entering the antenna.

Calculating the distance based on the slope from this data would result in unreliable measurements. Therefore, we propose to use a Fourier transformation $\mathcal{F}(\Phi)$ to get frequency f_Φ of phase shifts in Φ utilizing a Fast Fourier Transformation (FFT). f_Φ is proportional to the slope of the saw teeth in Φ. Figure 3 shows the result of a FFT over the data represented in Figure 2. The highest peak represents f_Φ. Due to the noise

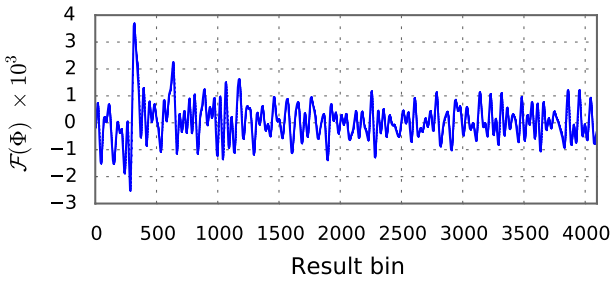

Fig. 3. FFT over raw phase response Φ

in Φ, caused by measurement errors, the FFT also generates peaks for other harmonic frequencies included in the phase response. This causes errors while detecting the peak of f_φ.

According to the Wiener-Khintchine theorem [13], the noise of a periodic signal can be suppressed by calculating the auto correlation of the noise affected signal. Equation 6 give the auto correlation $\Psi_{\Phi\Phi}(j)$ of a time discrete signal Φ.

$$\Psi_{\Phi\Phi}(j) = \sum_n \Phi_n \cdot \Phi_{n-j} \tag{6}$$

The auto correlated phase response results in an attenuated sine wave $\Psi_{\Phi\Phi}$. In $\Psi_{\Phi\Phi}$ the phase information of Φ is lost but the frequency information is preserved. Loosing the phase information does not harm the distance calculation as the distance is proportional to f_Φ. As this frequency is preserved the frequency $f_{\Psi_{\Phi\Phi}}$ of $\Psi_{\Phi\Phi}$ is equal to f_Φ.

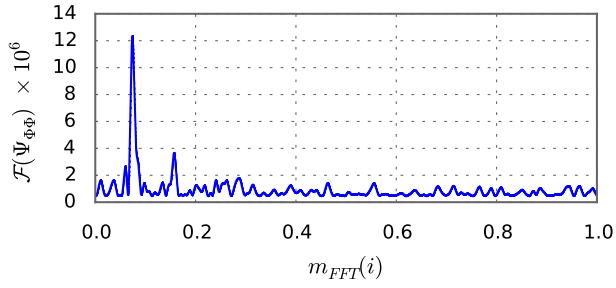

Fig. 4. FFT over auto correlated phase response $\Psi_{\Phi\Phi}$

The Wiener-Khintchine theorem also implies that the Fourier-transformed $\mathcal{F}(\Psi_{\Phi\Phi})$ of $\Psi_{\Phi\Phi}$, called PSD, is always positive and real. Figure 4 shows $\mathcal{F}(\Psi_{\Phi\Phi})$ calculated from the same data as in Figure 3. In $\mathcal{F}(\Psi_{\Phi\Phi})$ the peak of the distance is much more dominant and therefore much easier to detect.

The height of the peak of $\mathcal{F}(\Psi_{\Phi\Phi})$ can be used as a Distance Quality Factor (DQF) for the measurement, see Equation 7.

$$DQF = max(\mathcal{F}(\Psi_{\Phi\Phi})) \tag{7}$$

The more noise affects the signal, the lower the peak becomes. This is because the spectral power is distributed over more phase shift frequencies.

As the measured values are discrete in time and value, we can use a FFT to calculate $\mathcal{F}(\Psi_{\Phi\Phi})$. So from now on it is called $FFT_{\Psi_{\Phi\Phi}}(i)$. By adjusting the window size of the FFT, it is possible to adjust the accuracy and complexity of our calculations. This allows us to perform all calculations even on an 8 bit micro controller. The index i where $FFT_{\Psi_{\Phi\Phi}}(i)$ has its highest peak is called i_{max}. Depending on the window size of the FFT the value of i_{max} differs for the same distance. To correct this we use the scaling function 8.

$$m_{FFT}(i) = i \cdot \frac{2}{N} \tag{8}$$

Here, N is the window size of the FFT. The value of $m_{FFT}(i)$ lies between 0 and 1 for all values of N. Therefore, the chosen window size does not affect the following calculations.

To calculate the distance d between the two nodes Equation 9 is used.

$$d = d_{max} \cdot m_{FFT}(i_{max}) + d_{offset} \tag{9}$$

Here, d_{offset} results from characteristics of the antenna and the connections on the circuit board. d_{offset} can be determined by measuring a certain distance and subtracting the measured distance from the actual distance. This has to be done only once for each node because d_{offset} is hardware dependant and constant over time. d_{max} is the maximum measurable distance.

$$2 \cdot d_{max} = \frac{\lambda_{\Delta f}}{2} \tag{10}$$

Equation 10 results from the Nyquist-Shannon-Theorem. The theorem states that at least two measured points are needed to reconstruct the signal. For our system this implies that we need at least two measurements of the phase difference between two phase shifts to be able to measure f_φ. The other factor of two results from the AR method because the signal has to travel the real distance twice. We use $\Delta f = 500\,kHz$ which has $\lambda_{\Delta f} = 600m$. Therefore we are able to measure a distance $d_{max} = 150\,m$.

V. Evaluation

For the evaluation, we measured the distance between an initiating node and an AR. We sampled only the distance to one reflector, we did not calculate relative positions. For this, multiple reflectors would have been needed.

A. Test Setup and Scenarios

The method proposed in this paper has been implemented on an updated version of the INGA sensor node [3]. This platform consists of a micro controller *ATmega1284p* by *Atmel* and a standard IEEE 802.15.4 transceiver chip, *AT86RF233*, by the

TABLE I
TEST PARAMETER SETS

	A	B	C
TX Power	+4 dBm	-17 dBm	
$\mathbf{f_{start}}$	2400 MHz		2483 MHz
$\mathbf{f_{stop}}$	2500 MHz		
$\mathbf{f_{step}}$	500 kHz		

same manufacturer. This platform is not specially designed for phase measurements but is a general purpose wireless sensor node.

We conducted measurements with our system and compared our implementation with the Ranging Toolbox (RTB) by *Atmel* in different environments to get a realistic result of the performance.

Measurements have been recorded in four scenarios representing different use cases:

Basement: Measurements in the basement of an office building are expected to be influenced by harmful effects of reflection and multipath propagation of radio signals. The walls are made of concrete and steel.

Office corridor: The measurements in a long office corridor have been taken during a working day which means that a lot of users occupied the 2.4 GHz band with IEEE 802.11 communication as well as other IEEE 802.15.4 devices.

Apartment: Similar to the corridor there are a lot of IEEE 802.11 devices but in contrast to the office corridor rooms in an apartment are much smaller and therefore reflection might be challenging.

Park: For evaluating the outdoor performance in absence of other devices using the 2.4 GHz frequency band, open air measurements have been performed in a park.

For testing the performance of InPhase, we mounted a sensor node 2 m above ground on a rollable table. A second stationary node has been mounted at the same height on a wall for indoor measurements or on a pole for measurements in the park.

In order to compare the results with the existing system, we also conducted the same measurements sequentially with the RTB. The hardware is the evaluation kit *REB233CBB* by *Atmel*. The micro controller on the board is an *ATxmega256A3*, also manufactured by *Atmel*.

The reference of the distance was determined using a laser rangefinder. The accuracy is typically $\pm$ 1 mm, in the worst case (e. g. bright sunlight) $\pm$ 20 mm at 150 m.

B. Measurement parameters

In each scenario, we took 50 data samples every 5 m except for the **Apartment** where measurements were taken every 1 m. Due to space constraints, the maximum distance that could be measured have been 20 m in the **Basement**, 49 m in the **Office corridor**, 7 m in the **Apartment** and 130 m in the **Park**. As low distances are harder to measure due to a very low frequency in the phase response we performed additional measurements at distances of 0.5 m, 1 m and 2 m.

We used several sets of measurement parameters for the radios, shown in Table I. These parameter sets are based on recommendations by the RTB user's manual [1] for different environments. While set **A** is recommended for outdoor measurements, the sets **B** and **C** are recommended for indoor scenarios with a high level of reflections and thus use low TX power in order to minimize the influence of reflections. The higher value for $\mathbf{f_{start}}$ in set **C** was chosen to avoid interference with WLAN in the **Office Corridor** and the **Apartment**. Parameter set **A** was used in all environments for InPhase. As these parameters have a critical impact on the performance we conducted every indoor measurement of the RTB also with set **A** for a fair comparison.

The parameters shown can be described as follows:

TX power: Transmission power of the radio, given in **dBm**. This parameter influences multipath propagation and maximum transmission range.

$\mathbf{f_{start,stop,step}}$*:* Starting at $\mathbf{f_{start}}$, phase measurements were taken at every $f = \mathbf{f_{start}} + i \cdot \mathbf{f_{step}}, f \leq \mathbf{f_{stop}}, i = 0, 1, 2, \ldots$.

Depending on the actual circuit of the antenna network, a constant offset d_{offset} will occur for each hardware platform. To get an accurate value for this error, we calculated the offset based on all distances measured by the sensor node. These distances were compared to the reference from the laser rangefinder. The median error of all measurements with respect to the reference is the needed constant offset d_{offset}. In our case, the median of all measurements on our platform was $d_{offset,INGA} \approx 1.09\,\mathrm{m}$. Measurements with the RTB showed, that on this system, a medium error of 10.3 cm was detected, which has been set as $d_{offset,RTB} = 10.3\,\mathrm{cm}$.

C. Evaluation of Distance Quality Factor

The Distance Quality Factor (DQF) gives the quality of a measurement and enables the system to determine whether to trust the measurement or not. We compare our DQF – the height of the peak of $\mathcal{F}(\Psi_{\Phi\Phi})$ – to the DQF of the RTB. The DQF of the RTB is a value between 0 and 99, where 99 indicates a good measurement and 0 one with bad quality.

The following evaluation shows how the two DQFs perform in classifying whether a measurement has a higher error than $1\,m$ or not. This is in applications like localization of geriatric patients a reasonable tolerance for the position. Measurements more accurate than $1\,m$ are considered valid, others are invalid. To make this decision we use a threshold at a certain value. To determine this threshold, five different quality criteria are used:

Sensitivity: This parameter describes the ratio of accepted valid measurements over all valid measurements. A higher sensitivity indicates a better quality factor.

Specificity: This parameter describes the ratio of dropped invalid measurements over all invalid measurements. If this value is high many invalid measurements are identified and dropped by the quality factor.

Positive Predictive Value (PPV): This parameter describes the ratio of valid measurements over all accepted measurements. A high value indicates that only few invalid

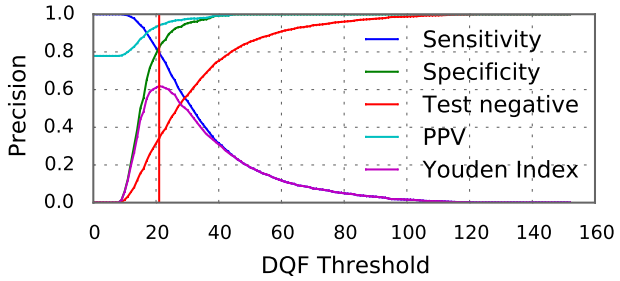

(a) InPhase, parameter set **A**

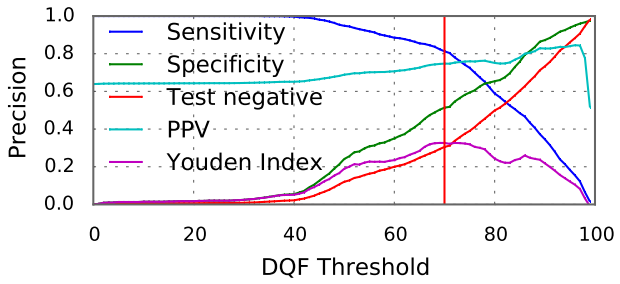

(b) RTB, parameter set **A-C**

Fig. 5. Quality criteria over DQF for InPhase and the RTB.

measurements are accepted. Having many invalid measurements in the accepted ones, decreases the overall quality of the measurement.

Test Negative: This parameter describes the ratio of dropped measurements over all measurements. If this value is high, it takes long until a valid measurement is performed because most measurements are dropped.

Youden Index [14]: This index is a combination of sensitivity and specificity. Equation 11 shows how the Youden index is to be calculated.

$$YoudenIndex = sensitivity + specificity - 1 \qquad (11)$$

The higher this value is, the better the quality factor and the threshold are able to separate valid and invalid measurements.

We propose to use the Youden index to define a threshold for valid measurements because it is a trade-off between sensitivity and specificity. For the graphs in Figure 5(a) and 5(b) the measurements of all test scenarios were combined to get an overall performance of the system. For results from the RTB with the recommended settings, we used the according parameter set for each scenario and combined them afterwards.

Figure 5(a) shows the five quality criteria over the DQF-threshold. It strengthens that the Youden index gives a good threshold. At the red vertical line – the maximum of the Youden index – all quality criteria have a high value but the test negative is still quite low. The maximum of 0.62 is at a DQF of 21.

Figure 5(b) shows the quality criteria for the RTB with the settings proposed by *Atmel*. It shows hardly any change below a DQF of 40. This is because the RTB only returns very few

TABLE II
DQF THRESHOLD

	InPhase, **A**	RTB, **A-C**	RTB, **A only**
Sensitivity	.79	.81	.85
Specificity	.83	.51	.50
Test Negative	.34	.31	.22
PPV	.94	.75	.87
max. Youden Index	.62	.33	.35
DQF Threshold	21	70	74

measurements with a DQF below 40. The Youden index is not continuously falling, there is a local minimum at 83. The PPV shows a local minimum at the same point. This local minimum results in the fact that measurement series with a higher DQF threshold may have more falsely accepted measurements than series with a lower DQF threshold.

Our proposed DQF does not show such behavior. Test negative is continuously rising while the Youden index is continuously falling after its maximum. In comparison to our system's DQF, the DQF of the RTB results in much more spread and a lower Youden index. Therefore our DQF is more suitable to separate valid from invalid measurements.

Table II shows the values of the different quality criteria for the maximum of the Youden index. The first column contains the values of our proposed system. In the second column the combined values for all recommended parameter sets for the RTB are shown. The last column shows the results of the RTB with our parameters. A PPV of 0.94 for InPhase indicates that of the measurements that are classified as valid by our DQF almost all have an error smaller than 1 m.

D. Results of Distance Estimation

The results are presented as follows: First, we compare the different parameter sets for the RTB and how they influence the performance. Afterwards, we compare the overall performance of InPhase to the RTB as current state of the art for AR distance estimation.

For our system we present results with applied DQF cut-off, hence only measurements with a DQF $>$ 21 are taken into account. However, for the RTB we present results without applied cut-off. Our experiments show that an internal cut-off is already applied by the RTB. During measurements the RTB does not return measurements at a constant rate but sometimes halts without returning data, indicating that it drops invalid measurements.

We present the results as box-and-whisker plots. The red line always indicates the median error, while the whiskers show the 1.5 interquartile range.

1) Comparison of Parameter Sets: For the RTB, we compared the results of measurements which have been made with the manufacturer's recommendations (Parameter set **A** to **C**) and our settings (Parameter set **A** exclusively) in Table I.

Figures 6(a) and 6(b) show the results of measurements for the **Office Corridor** scenario with the RTB for parameter set **C** and **A**, respectively. With the settings recommended by *Atmel*, it was not possible to get a valid result for all distances. At

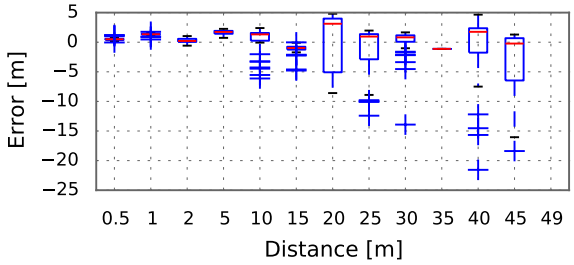

(a) Parameter set **C** (recommended)

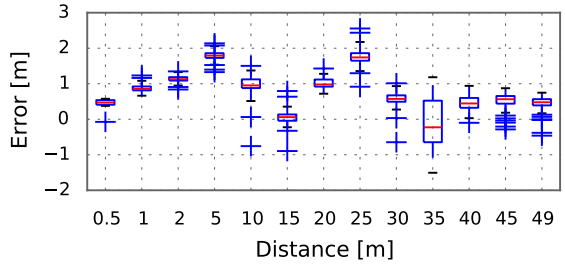

(b) Parameter set **A**

Fig. 6. Measurements taken with RTB in **Office Corridor** scenario

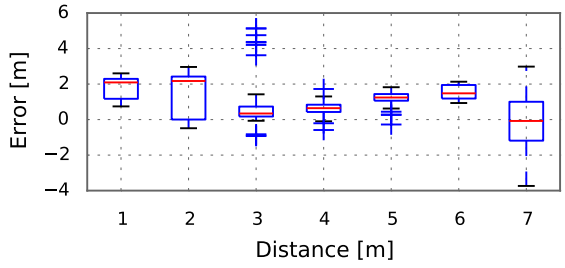

(a) Parameter set **C** (recommended)

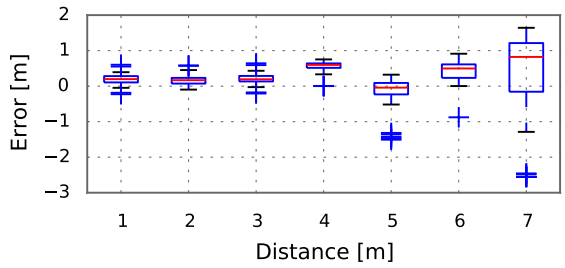

(b) Parameter set **A**

Fig. 7. Measurements taken with RTB in **Apartment** scenario

49 m no reliable communication between nodes was possible with parameter set **C**, hence no results could be obtained.

Figures 7(a) and 7(b) show the same effect in the **Apartment** scenario; the variance of the results decreases as well.

Figures 8(a) and 8(b) show the results from measurements taken in the **Basement** scenario. For these, parameter sets **B** and **A** have been used. Although *Atmel* proposes a low transmission power to minimize errors resulting from reflection, with a increased TX power of $+4\,\mathrm{dBm}$ instead of $-17\,\mathrm{dBm}$, the variance of results is lower. Figure 8 shows that the result can be improved using a higher transmission power with

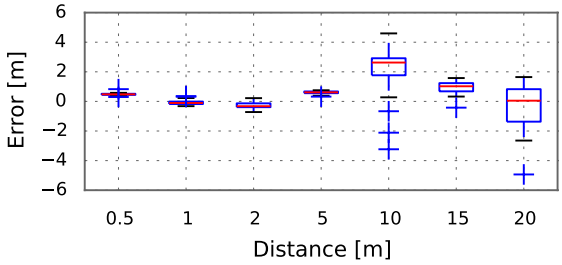

(a) Parameter set **B** (recommended)

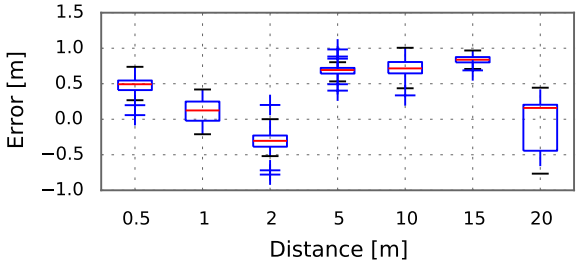

(b) Parameter set **A**

Fig. 8. Measurements taken with RTB in **Basement** scenario

an otherwise unchanged system. The variance of the results decreases clearly.

2) Results in dedicated scenarios:

Park: The results of the **Park** scenario are shown in Figure 9(a) and Figure 9(b). In each figure, the upper and lower diagrams show the same data, but with a different scaling. InPhase shows lower variance in results than the RTB but occasional outliers with large errors. At a distance of 60 m both systems indicate problems with the measurement. Our system dropped all measurements as invalid while the RTB reported distances with large errors. We assume environmental conditions to cause this effect.

Office Corridor: Similar to the **Park** scenario, the variance of the measurement errors for InPhase is smaller than for the RTB but feature occasional outliers that were not detected by the DQF classification. The results for the RTB are shown in Figure 6(b), the results for our system with two scales are in Figure 10. Despite the outliers InPhase's median error outperforms the RTB.

Apartment: In the **Apartment** our system shows the same properties as in the previous measurements, see Figure 11. The RTB profits from our custom parameter set **A**, see Figure 7.

Basement: In this scenario, our system outperforms the RTB, see Figure 12 and Figure 8. However, this environment is more demanding and both systems show larger overall errors.

3) Error of Measurement: To evaluate the performance of our system against the proposed Ranging Toolbox (RTB) by *Atmel*, we calculated the median error of all measurements. For each system two results are presented. The first result shows the median error without applying any DQF cut-off, see Table III. Our system outperforms the RTB without any applied cut-off, although the RTB already dropped measurements internally. Parameter set **A** results in a smaller error even when

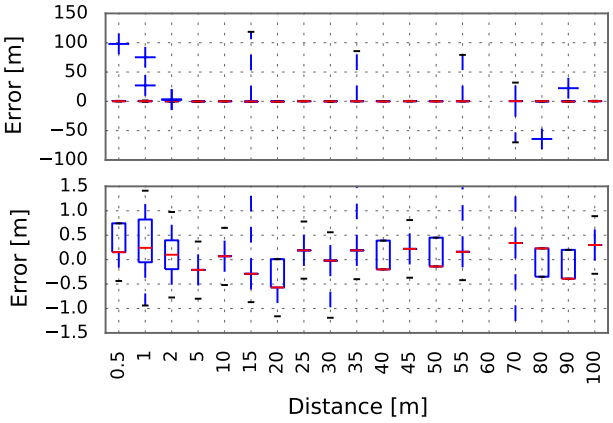

(a) InPhase, parameter set **A**

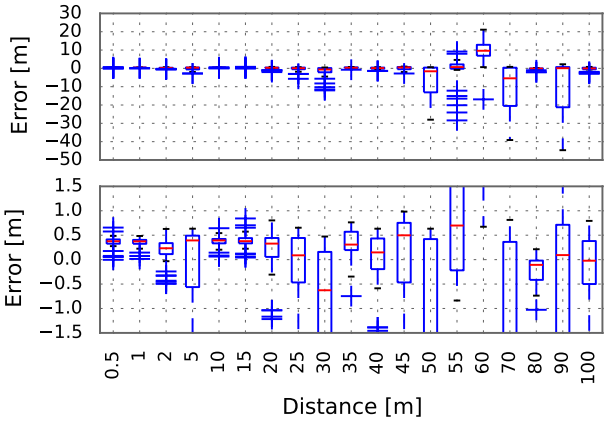

(b) RTB, parameter set **A**

Fig. 9. Measurements taken with InPhase and RTB in **Park** scenario. Both graphs of (a) and (b) show the same data with different scales to improve readability.

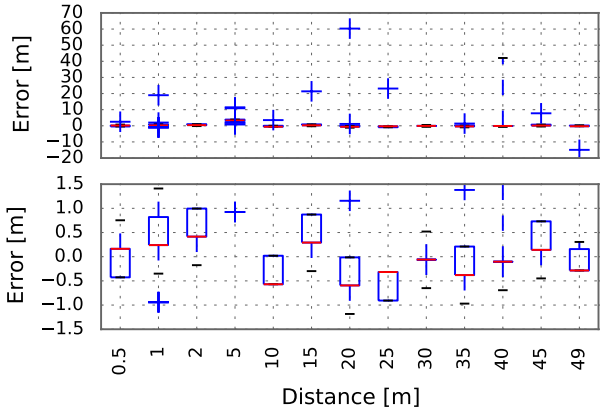

Fig. 10. Measurements taken with InPhase in **Office Corridor** scenario. Both graphs show the same data, with different scales to improve readability.

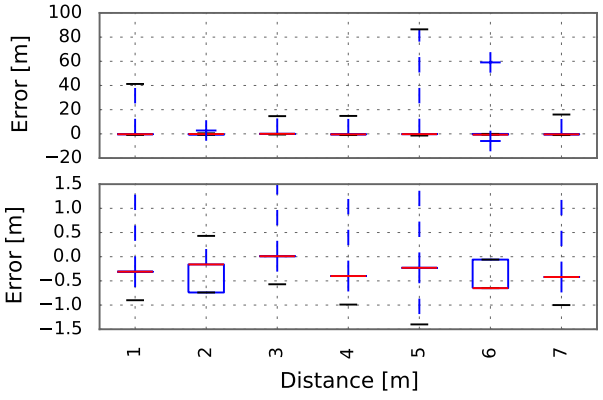

Fig. 11. Measurements taken with InPhase in **Apartment** scenario. Both graphs show the same data with different scales to improve readability.

TABLE III
MEDIAN ERROR OF MEASUREMENT

	InPhase	**RTB, *A-C***	**RTB, *A only***
Median Error	0.40 m	0.59 m	0.50 m
# Measurements	2172	1931	2195

using the RTB. The second result shows the median error with cut-offs applied for both systems, see Table IV. InPhase profits the most from this operation and can reduce the median error to 30 cm. Both results show, that our system is more accurate whether the DQF cut-off is applied or not.

E. Power Consumption and Duration

We compared the current of our system and the RTB. Although different hardware platforms are used, it is possible to get an impression of the differences occuring for both systems. To perform the measurements, a shunt of 0.4 Ω has been inserted in the power line. The voltage over this resistor has been sampled with a frequency of 10 kHz.

We captured the current of the whole node, including all modules. Due to different controllers on the boards, the

TABLE IV
MEASUREMENT ACCURACY USING DQF THRESHOLD

	InPhase, **A**	RTB, **A-C**	RTB, **A only**
Median Error	0.30 m	0.45 m	0.47 m
% accepted measurements	68.55 %	70.64 %	79.54 %
% gain with DQF	25.00 %	23.73 %	6.00 %

absolute values of the current shown in Figure 13 are not meaningful, but they reveal the differences of the methods used by the RTB (*REB233CBB*) and InPhase. The CPU on the evaluation board and the radio frontend result in a higher power consumption than in our system.

In Figure 13, three states of the measurement process can be identified. Before the measurement cycle, the controller and radio are in idle mode, ready to receive data. The initiating node sends commands to the AR. When the measurement starts, the AR receives the command as well as needed parameters to configure the measurement process. The reception of the data packets results in changing current consumption,

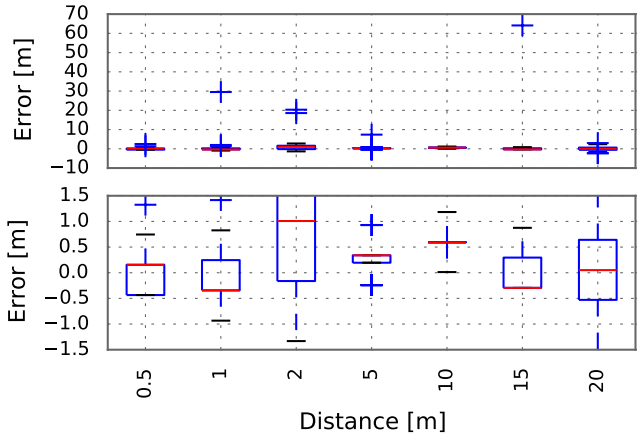

Fig. 12. Measurements taken with InPhase in **Basement** scenario. Both graphs show the same data with different scales to improve readability.

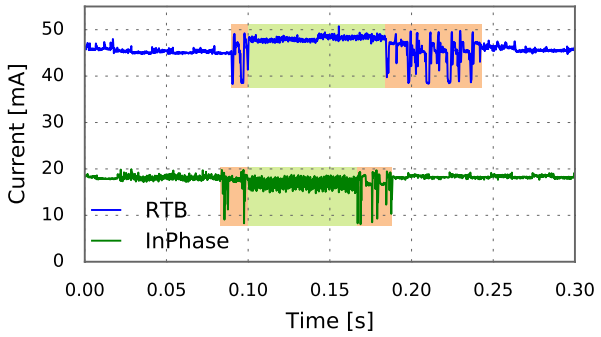

Fig. 13. Current of both types of AR nodes

since the radio switches its mode during data transfers. During the actual distance measurement, the current is constantly slightly higher or lower than in the idle state, depending on the implementation of the hardware and the controllers. The part after the measurement reveals differences between the RTB and our implementation. The RTB probably transmits raw data to the initiating node while we perform more calculations of results on the AR itself, which means that fewer data packets need to be transmitted. This reduces the time for the complete measurement cycle.

VI. Conclusion

In this paper we presented InPhase. A system for distance measurements that can be employed to upgrade the feature set of wireless sensor nodes. In contrast to other systems, we do not need any extra hardware but only the regular transceiver chip used for the communication. Thus, no additional cost arises and the feature can be added to an IoT deployment by updating the software only.

A localization system relies on accurate distance measurements for further processing steps as trilateration. Therefore, we focused on optimizing this measurement. The distance estimation is based on the measurement of phase differences between the received signal and a locally generated reference signal. To overcome the hard synchronization requirements of the reference signals we use the Active Reflector (AR) method. We proposed a novel approach to determine the distance from the measured phase differences utilizing the Power Spectral Density (PSD). Utilizing the PSD allows us to fit the complexity of calculations to the underlying hardware capabilities. Further, we demonstrated that the PSD allows to estimate a sample's quality with no extra calculation.

The results from our evaluation show that InPhase has a median distance error of 0.3 m over all measurement scenarios after applying a DQF threshold. With this result, our system outperforms the Ranging Toolbox (RTB) by 33 %. The evaluation of the DQF also shows that our DQF is more reliable than the one of the RTB.

Although our system already provides a dependable and accurate distance estimation for localization applications, it still can be improved in the future. A reliable recognition of disturbed links would help to avoid measurement errors. Further, frequencies that have lots of interference could be skipped to speed up measurements.

References

[1] Atmel Corporation, San Jose. *Atmel AVR2150: RTB Evaluation Application – User's Guide*, 8441a-avr-02/2013 edition, Feb. 2013.

[2] A. Boukerche, H. A. Oliveira, E. F. Nakamura, and A. A. Loureiro. Localization systems for wireless sensor networks. *Wireless Commun.*, 14(6):6–12, Dec. 2007.

[3] F. Büsching, U. Kulau, and L. Wolf. Architecture and evaluation of inga - an inexpensive node for general applications. In *Sensors, 2012 IEEE*, pages 842–845, Taipei, Taiwan, oct. 2012. IEEE.

[4] A. Dunkels, B. Gronvall, and T. Voigt. Contiki - a lightweight and flexible operating system for tiny networked sensors. In *Local Computer Networks, 2004. 29th Annual IEEE International Conference on*, pages 455–462, Nov 2004.

[5] V. Honkavirta, T. Perala, S. Ali-Loytty, and R. Piche. A comparative survey of wlan location fingerprinting methods. In *Positioning, Navigation and Communication, 2009. WPNC 2009. 6th Workshop on*, pages 243–251, Mar. 2009.

[6] W. Kluge and E. Sachse. System, method, and circuit for distance measurement between two nodes of a radio network, Feb. 4 2014. US Patent 8,644,768.

[7] A. Malekpour, T. Ling, and W. Lim. Location determination using radio frequency rssi and deterministic algorithm. In *Communication Networks and Services Research Conference, 2008. CNSR 2008. 6th Annual*, pages 488–495, May 2008.

[8] T. Nowak, M. Hierold, A. Koelpin, M. Hartmann, H.-M. Troger, and J. Thielecke. System and signal design for an energy-efficient multi-frequency localization system. In *Wireless Sensors and Sensor Networks (WiSNet), 2014 IEEE Topical Conference on*, pages 55–57, Jan. 2014.

[9] M. Pelka, C. Bollmeyer, and H. Hellbrück. Accurate radio distance estimation by phase measurements with multiple frequencies. In *2014 International Conference on Indoor Positioning and Indoor Navigation*, Oct. 2014.

[10] N. B. Priyantha, A. K. Miu, H. Balakrishnan, and S. Teller. The cricket compass for context-aware mobile applications. In *Proceedings of the 7th Annual International Conference on Mobile Computing and Networking*, MobiCom '01, pages 1–14, 2001.

[11] A. Savvides, C.-C. Han, and M. B. Strivastava. Dynamic fine-grained localization in ad-hoc networks of sensors. In *Proceedings of the 7th Annual International Conference on Mobile Computing and Networking*, MobiCom '01, pages 166–179, New York, NY, USA, 2001. ACM.

[12] H. Schantz. Near field phase behavior. In *Antennas and Propagation Society International Symposium, 2005 IEEE*, volume 3B, pages 134–137 vol. 3B, July 2005.

[13] N. Wiener. *Extrapolation, Interpolation, and Smoothing of Stationary Time Series*. The MIT Press, 1964.

[14] W. J. Youden. Index for rating diagnostic tests. *Cancer*, 3(1):32–35, 1950.